Spectroscopic studies of $5d_{3/2}nd\ ^1D_{0,2}$ autoionization lines of barium under collision with rare gases

K. Afrousheh,* M. Marafi, J. Kokaj, Y. Makdisi, and J. Mathew
Department of Physics, Kuwait University, P.O. Box 5969, 13060 Safat, Kuwait
(Received 4 April 2012; published 29 May 2012)

The spectroscopic behavior of $5d_{3/2}nd$ ($^1D_0$ and $^1D_2$) autoionizing Rydberg series of barium was studied under collision with rare gases. The series members from $n = 8$ to $n = 64$ were observed using two-photon excitation of the two valence electrons in the $6s^2\,^1S_0$ ground state of barium. The barium vapor was produced in a heat-pipe-like oven, and a tunable dye laser pumped by an excimer laser was used as the excitation source. The obtained spectral data have Beutler-Fano profiles. These spectral lines were investigated when inert gases Ar, Kr, and Xe at different pressures were introduced into the oven as perturbing gases. The collision-induced line shifts were measured and the shift parameters for the even-parity $5d_{3/2}nd\ ^1D_0$ and $5d_{3/2}nd\ ^1D_2$ (n = 8–35) autoionizing states were extracted from the data. The collision-induced change in the spectral line shape at different Xe pressure was also explored.

DOI: 10.1103/PhysRevA.85.052517 PACS number(s): 32.70.Jz, 32.80.Zb

I. INTRODUCTION

The singly and doubly excited Rydberg states of alkaline-earth-metal atoms have been studied extensively in the past [1,2]. In doubly excited atoms two valence electrons are simultaneously excited. In this case, if the energy of the excited configuration is above the first ionization limit, it can result in the autoionization process: One of the electrons decays to a lower-lying energy state while ionizing the other electron by an exchange of energy. This coupling between the two excited electrons causes the autoionizing states to have distinct properties from those of other excited states below the first ionization threshold. For example, autoionization spectral lines usually have large linewidths compared to normal singly and doubly excited lines. In addition, since the final configuration involves two interacting excited electrons, the shapes of autoionization spectral lines of unperturbed atoms depend on the excitation scheme. The isolated core excitation (ICE) technique [3], for instance, results in spectral lines that are approximately symmetric with a Lorentzian profile [4]. In the ICE technique, the two valence electrons are excited separately in stepwise laser excitations using a few different wavelengths. The interaction between electrons only shifts and broadens the spectral lines, but it results in symmetric Lorentzian line shapes.

Asymmetric spectral line profiles are also possible in such excitation schemes as vacuum ultraviolet (vuv) absorption spectroscopy [5] or two-photon excitation to the final autoionizing Rydberg states [6]. For unperturbed atoms, autoionizing lines with asymmetric Beutler-Fano profiles have been observed in both methods. In the experiments presented here, two-photon excitation was used to populate autoionizing series converging to the $5d_{3/2}$ state of Ba^+. This excitation scheme has also been used previously to excite autoionizing resonances in the energy range between $5d_{3/2}$ and $5d_{5/2}$ states of Ba^+ in order to measure photoionization spectra in this region [6]. In these situations the ground-state configuration is changed to an autoionizing configuration at once. The amplitudes of the excitation from the ground state to both doubly excited autoionizing states and degenerate continuum states are nonzero. The interference between these excitation amplitudes is responsible for the shape of the spectral line profiles. A spectral line, therefore, contains information regarding the excitation scheme as well as the properties of the excited state such as its linewidth and decay rate or lifetime.

Studying changes in spectral line properties caused by collisions provides additional information regarding the atom under investigation and its environment. For instance, measurements of the collision broadening and shift of spectral lines contain information regarding interatomic forces [7]. Furthermore, collisions whether between same species or between different species play an important role in decoherence of atomic systems in the gas phase [8]. Therefore, in addition to spectroscopic importance, understanding the influence of collisions on atomic spectra is also valuable for coherent control experiments [9]. We have previously reported the line broadening and shift of singly and doubly excited Rydberg states of calcium and barium with Ar, Kr, and Xe perturbers [10,11]. Other groups have performed experimental as well as theoretical work on normal and autoionizing Rydberg states of alkaline-earth-metal atoms. In the case of autoionization lines, most of the research has focused on mapping their spectra [12–15], and in some cases on configuration interactions among these states [16–18]. There is a lack of experimental and theoretical work on the behavior of these states under collision with other species.

In this paper, we extended the observed resonance spectral lines of the $5d_{3/2}nd\ ^1D_0$ and $^1D_2$ autoionizing series of Ba to $n = 64$. Previously, members of this series were observed up to $n = 30$ for $J = 0$ and $J = 2$ and up to $n = 44$ for other levels with different angular momentum quantum number [12]. The change in the energy level position and line shape of these states when under collision with rare gases (Ar, Kr, and Xe) is also reported. As these states are reached through a two-photon absorption process, the excited state will have the same parity as the ground state due to selection rules. In the case of barium the ground state is $6s^2\,^1S_0$, which has even parity. Utilizing the two-photon excitation enables us to excite the ground-state electrons to energy states of even parity with a total angular momentum quantum number of $J = 0$ and $J = 2$.

*Corresponding author: k.afrousheh@ku.edu.kw

II. EXPERIMENTAL DETAILS

The experiments were performed inside two heat-pipe-like ovens with a thermionic diode detection system as described in our previous publications [10,11]. The schematic of the experimental setup is given in Fig. 1. One heat-pipe oven is used as the reference cell (RFC) and the other as the high-pressure cell (HPC). In both cells the barium vapor was produced through heating the cells to 800 °C. A quartz window, which was water cooled, was used to provide optical access into each cell. In order to prevent Ba condensation on this window, the cells were filled with helium at a pressure of 5 mbar as a buffer gas. In addition, the high-pressure cell was filled with different inert gases whose pressures were changed in a controlled manner in different experiments. The perturbation of the spectral lines due to 5 mbar of helium was negligible in our experiments. The $5d_{3/2}nd\ ^1D_0$ and $5d_{3/2}nd\ ^1D_2$ autoionizing Rydberg states of barium atom were produced by two-photon excitation of the two $6s^2$ electrons of the ground state. A tungsten rod at the center of each oven was used for detecting the ions produced through ionization or autoionization of Rydberg states [19]. The tungsten rod was biased at 9 V with respect to the grounded cell body. The resulting signal was averaged for every ten laser pulses using two identical boxcar averagers.

The energies of the $5d_{3/2}nd$ series for $n = 8$ to 64 are within the range of 43 000 cm^{-1} to 47 000 cm^{-1} above the ground state, which goes up to ~4000 cm^{-1} above the first ionization limit. Two-photon absorption of a laser with a wavelength ranging from 420 to 470 nm is able to populate these autoionizing states. The excitation source was an excimer pumped dye laser with a repetition rate of 10 Hz, having a pulse duration of 15 ns and linewidth of 0.2 cm^{-1}. The dye laser wavelength was scanned in 0.0009-nm steps to excite different atomic resonances. As the laser frequency was scanned, different members of the $5d_{3/2}nd$ as well as some lines belonging to $5d_{3/2}ns$ and $5d_{3/2}ng$ were observed. The laser beam was focused into the Ba cells close to the tungsten rod and aligned in order to maximize the detector signal corresponding to collision produced ions. Power broadening of spectral lines was minimized through proper attenuation of the laser beam in order to improve the sensitivity of our experiments to additional line broadening due to collisions with perturber gases.

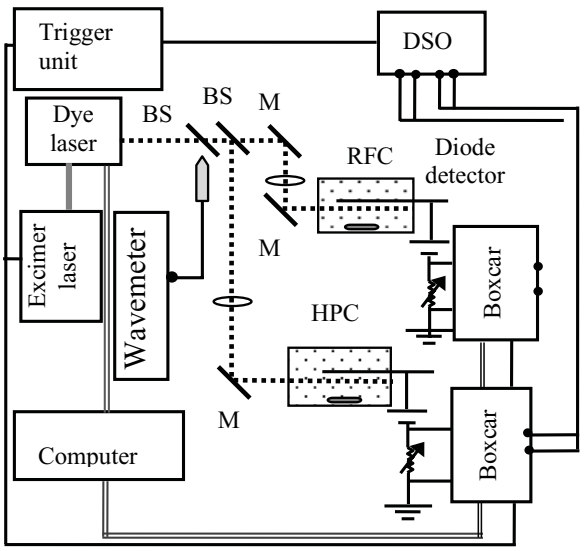

FIG. 1. Schematic diagram of the experimental setup. The abbreviations used are M: mirror, BS: beam splitter, DSO: digital storage oscilloscope, RFC: reference cell, and HPC: high-pressure cell.

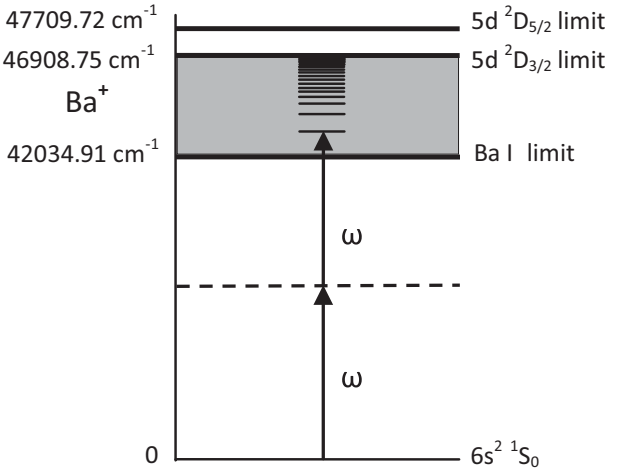

FIG. 2. Atomic barium energy level diagram, showing the relevant energy levels in the two-photon excitation process.

III. RESULTS AND DISCUSSION

A schematic of the excitation process from the ground state to autoionizing Rydberg states via a virtual intermediate state is given in Fig. 2. Part of the atomic spectra obtained from the RFC corresponding to a fast laser scan is represented in Fig. 3. This data were used to find the experimental energies of the members of the $5d_{3/2}nd\ ^1D_J$, $J = 0$ and $J = 2$ series relative to the ground state. The energy values measured this

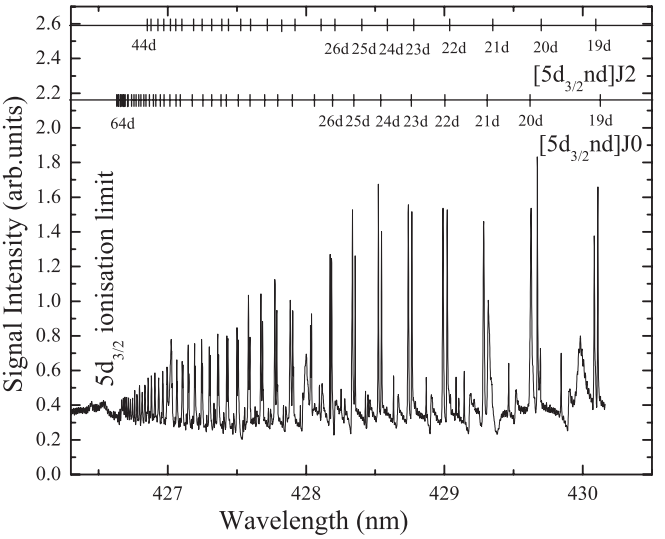

FIG. 3. The even-parity autoionizing states of barium near the $5d_{3/2}$ ionization limit.

TABLE I. Shift rate of $[5d_{3/2}nd\ ^1D_J]$ $J = 0$ autoionizing resonances of barium.

n	Energy (cm^{-1}) Camus *et al.*[a]	Energy (cm^{-1}) Present work	Shift rate [cm^{-1} (r.d.)$^{-1}$]		
			Ar at 100 mbar	Kr at 100 mbar	Xe at 100 mbar
8	43281.67	43281.81	0.0	2.1 ± 1.1	4.3 ± 0.9
9	44324.10	44324.39	3.5 ± 0.1	2.8 ± 0.7	6.3 ± 0.9
10	44956.43	–	–	–	–
11	45397.82	45397.82	3.6 ± 0.0	5.2 ± 0.9	7.5 ± 1.3
12	45691.69	45692.02	17.2 ± 1.4	39.7 ± 1.5	82.6 ± 1.5
13	45918.28	45917.94	26.4 ± 0.0	41.6 ± 1.5	72.5 ± 0.9
14	46080.30	46080.46	10.1 ± 1.3	15.2 ± 0.0	17.7 ± 0.6
15	46197.60	46193.22	9.6 ± 1.1	22.2 ± 0.9	36.9 ± 0.9
16	46308.92	46308.94	13.5 ± 1.1	21.8 ± 1.3	42.7 ± 1.5
17	46387.75	46387.74	14.1 ± 1.3	18.1 ± 1.2	30.1 ± 1.4
18	46451.99	46452.47	17.3 ± 1.1	20.6 ± 1.3	41.8 ± 1.4
19	46500.75	46499.99	13.9 ± 0.9	18.5 ± 1.8	32.4 ± 0.9
20	46551.76	46551.86	17.5 ± 1.1	23.3 ± 0.0	46.7 ± 1.6
21	46588.72	46588.98	13.8 ± 1.7	24.3 ± 1.9	45.9 ± 1.7
22	46620.54	46620.62	10.9 ± 1.4	25.5 ± 0.9	43.8 ± 1.9
23	46647.74	46647.77	16.1 ± 1.1	25.1 ± 1.1	46.8 ± 0.0
24	46671.30	46671.68	14.7 ± 0.8	24.5 ± 1.4	44.9 ± 1.1
25	46691.74	46691.78	11.7 ± 0.6	22.1 ± 1.5	33.5 ± 1.3
26	46709.58	46709.72	11.7 ± 0.6	22.6 ± 1.0	43.2 ± 0.1
27	46729.02	46728.94	17.4 ± 1.1	24.8 ± 1.3	42.8 ± 0.2
28	46740.77	46741.10	17.6 ± 1.0	35.2 ± 1.8	51.1 ± 0.2
29	46752.90	46753.12	21.9 ± 1.4	30.8 ± 0.5	50.9 ± 0.0
30	46763.78	46763.81	13.7 ± 0.9	24.0 ± 0.5	54.9 ± 0.0
31	–	46774.13	13.1 ± 1.3	22.2 ± 1.3	41.6 ± 0.5
32	–	46783.03	13.1 ± 1.3	26.1 ± 1.3	37.7 ± 0.9
33	–	46791.04	11.8 ± 0.0	23.5 ± 0.0	44.3 ± 1.4
34	–	46798.48	11.8 ± 0.0	21.6 ± 1.5	39.2 ± .1.8
35	–	46805.09	17.0 ± 1.3	23.6 ± 0.0	45.5 ± 1.9

[a]Reference [12].

way for series members from $n = 8$ to $n = 35$ are given in Tables I and II (third column). For comparison, the energy values measured by Camus *et al.* [12] for $5d_{3/2}nd\ ^1D_J$, $J = 0$ and $J = 2$ series members for $n = 8$ to $n = 30$ are given in the second column of Tables I and II. The level energies obtained in our experiments are consistent with those reported by Camus *et al.* with one exception at $n = 15$. We did not observe any resonance near the energy value 46 197.6 cm^{-1} mentioned by Camus *et al.* for $J = 0$ level of $n = 15$ and identified this level at 46 193.23 cm^{-1}. This discrepancy has to be investigated with other experimental techniques. The newly measured energies of the series members from $n = 36$ up to $n = 64$ are listed in Table III (columns 2, 3, 5, and 7).

Using the two-photon absorption process with a single laser reduces the complexity of the experimental setup as fewer optical components are required and there is no need for synchronizing different lasers. However, the downside of the two-photon absorption process in exciting autoionizing states is the poor signal-to-noise ratio especially for higher noble gas pressures. The same excitation method was used previously by our group to study singly excited as well as doubly excited Rydberg series that lie below the first ionization limit of the alkaline-earth-metal atoms [11,20]. The normal trend is that the signal-to-noise ratio decreases in the order of singly excited, doubly excited, and autoionizing states. In case of autoionizing states the ion signal obtained with the thermionic diode detector has a sharp rise and a slowly decaying tail. The sharp rise is due to a sudden change in the space charge density around the tungsten rod, hence a sharp rise in the diode signal. The ions will gradually disappear and the diode signal decreases slowly.

Figure 4 presents a single resonance line corresponding to $5d_{3/2}15d$, $J = 0$, which reveals the details of the line shape of the spectral lines. Different traces in this figure are obtained from the RFC and the HPC with three different pressures of Xe as the perturbing gas. The asymmetric profile of the resonance line obtained in the RFC is of the Beutler-Fano shape. This line shape is caused by the coupling between the excited autoionizing state and the degenerate continuum state, and the width of this line depends on the strength of the coupling. The coupling itself is due to nonzero transition dipole moments in two-photon excitation for both excited and continuum states.

As seen in Fig. 4, the transition line shape deviates from the Beutler-Fano profile (the fitted curves) when the perturber gas (Xe) is introduced into the cell. The linewidth of the broadened transition and the profile of the spectral line depend on the detail of the interatomic potential. Without adequate knowledge of the interatomic potential the precise measurement of the collisional broadening of spectral lines

TABLE II. Shift rate of $[5d_{3/2}nd\ ^1D_J]$ $J = 2$ autoionizing resonances of barium.

n	Energy (cm^{-1}) Camus *et al.*[a]	Energy (cm^{-1}) Present work	Shift rate [cm^{-1} (r.d.)$^{-1}$]		
			Ar at 100 mbar	Kr at 100 mbar	Xe at 100 mbar
8	43153.98	–	–	–	–
9	44238.02	44238.09	2.1 ± 1.1	2.8 ± 1.1	2.8 ± 1.3
10	44900.27	44900.35	3.6 ± 0.0	10.8 ± 0.0	16.6 ± 0.9
11	45348.31	45348.94	11.4 ± 1.1	20.6 ± 1.5	28.0 ± 1.5
12	45663.75	45663.97	9.7 ± 0.8	30.7 ± 1.5	33.6 ± 1.1
13	45894.66	45894.93	10.6 ± 0.8	43.7 ± 1.5	67.9 ± 1.0
14	46064.53	46064.76	13.7 ± 0.9	69.4 ± 0.6	84.4 ± 0.9
15	46199.17	46199.54	15.1 ± 1.5	27.9 ± 1.6	36.0 ± 0.7
16	46296.94	46297.41	14.1 ± 1.3	23.0 ± 0.0	38.8 ± 1.1
17	46379.95	46380.29	12.9 ± 1.3	20.6 ± 1.3	27.0 ± 1.6
18	46445.68	46445.87	14.2 ± 1.3	21.9 ± 1.3	109.0 ± 0.6
19	46502.36	46502.45	14.7 ± 1.5	20.5 ± 1.4	39.7 ± 1.0
20	46546.72	46547.10	12.4 ± 0.8	20.4 ± 1.0	38.8 ± 1.6
21	46585.44	46585.47	26.7 ± 1.7	28.7 ± 0.8	46.7 ± 1.6
22	46617.36	46617.49	9.8 ± 1.0	18.7 ± 1.2	38.9 ± 1.6
23	46645.10	46645.33	9.7 ± 0.9	18.7 ± 1.2	35.0 ± 1.6
24	46669.69	46669.63	9.3 ± 1.0	15.6 ± 1.0	33.2 ± 1.1
25	46692.61	46692.43	13.2 ± 0.5	23.8 ± 1.1	41.0 ± 1.1
26	46708.31	46708.55	13.1 ± 0.5	14.5 ± 1.2	30.3 ± 1.8
27	46724.69	46724.85	15.0 ± 0.5	23.0 ± 0.3	35.2 ± 0.0
28	46738.65	46738.79	16.6 ± 1.5	22.7 ± 1.2	35.2 ± 0.0
29	46751.27	46751.74	12.4 ± 0.5	21.2 ± 1.7	23.5 ± 0.0
30	46762.65	46762.94	11.8 ± 0.1	21.9 ± 1.6	35.5 ± 0.2
31	–	46772.76	9.2 ± 1.3	17.0 ± 1.3	52.5 ± 1.5
32	–	46782.12	11.8 ± 0.0	15.7 ± 1.6	49.8 ± 0.9
33	–	46790.16	9.2 ± 1.3	21.6 ± 1.1	55.1 ± 1.1
34	–	46797.58	9.9 ± 1.1	24.9 ± 1.1	46.3 ± 1.3
35	–	46804.38	10.5 ± 1.3	20.9 ± 1.1	44.0 ± 1.3

[a]Reference [12].

through fitting the data with an appropriate function would be difficult. Considering the fact that the signal-to-noise ratio decreases for higher members of the Rydberg series, we limited our measurements to shift rates of spectral lines of the Rydberg series. The collision-induced changes to the line shapes of the autoionizing states and measurement of their broadening parameters are currently under more detailed investigation by our group.

The spectral line shifts of the $5d_{3/2}nd\ ^1D_J$ series for $J = 0$ and $J = 2$ for n ranging from 8 to 35 have been measured for Ar, Kr, and Xe perturbers at different perturber pressures. Plots of line shift versus perturber gas pressure for $5d_{3/2}19d\ ^1D_0$ and $5d_{3/2}19d\ ^1D_2$ are given in Fig. 5 as examples. There are two main reasons for the pressure shift of spectral lines. The first, which is the most important, is the elastic scattering of the Rydberg electron from the perturber atoms and is given

TABLE III. Term energies of $[5d_{3/2}nd\ ^1D_J]$ $J = 0, 2$ autoionizing resonances of barium (for $n = 36$ to 64) observed in the present work.

n	Term energy (cm^{-1})		n	Term energy (cm^{-1})	n	Term energy (cm^{-1})
	$J = 0$	$J = 2$				
36	46811.54	46810.95	46	46851.42	56	46871.18
37	46817.16	46816.57	47	46853.99	57	46872.67
38	46822.19	46821.70	48	46856.46	58	46873.95
39	46826.93	46826.43	49	46858.73	59	46875.23
40	46831.27	46830.77	50	46860.91	60	46876.33
41	46835.72	46835.23	51	46862.88	61	46877.51
42	46838.98	46838.68	52	46864.76	62	46878.50
43	46842.43	46842.13	53	46866.54	63	46879.49
44	46845.69	46845.40	54	46868.12	64	46879.59
45	46848.65	46848.36	55	46869.70		

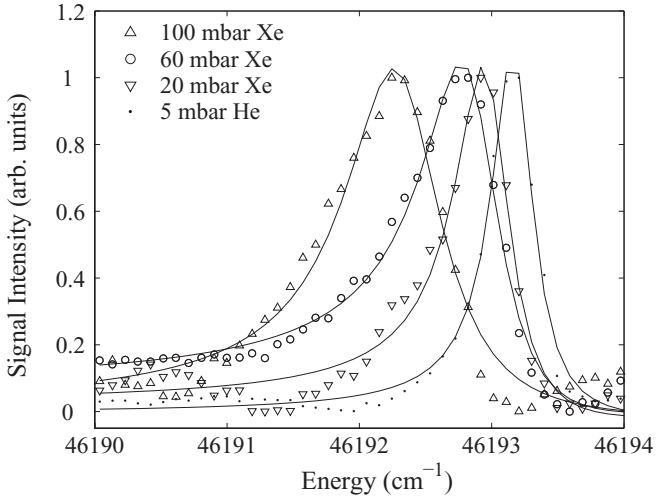

FIG. 4. Experimental data and the corresponding Beutler-Fano-fitted profile (solid curves) for the Ba $5d_{3/2}15d\ ^1D_0$ Rydberg transition with 5-mbar He in RFC, 20-mbar Xe, 60-mbar Xe, and 100-mbar Xe in HPC.

by $\Delta_{el} = 2\pi aN$, with a being the scattering length and N the number of perturbing atoms [2]. The second reason is the scattering of the ionic core of the Rydberg atom from the perturber atoms, which is given by $\Delta_{\text{ion}} = -\pi\alpha N(\frac{4}{3}\pi N)^{1/3}$ in which α is the polarizability of the perturber. Although the dependence of the line shift on the number of perturber atoms (N) is different for the two interactions, the line shift increases with increasing N. As seen in these graphs, the shift changes linearly with perturber gas pressure within the experimental errors, which agrees with the fact that elastic electron scattering is the dominant effect in the spectral line shift. Similar behavior was observed for other members of the series. In all cases, the shift values increase in the order of Ar, Kr, and Xe perturbers as the scattering lengths and the polarizabilities of these elements increase in the same order. Overall, the dependence of spectral

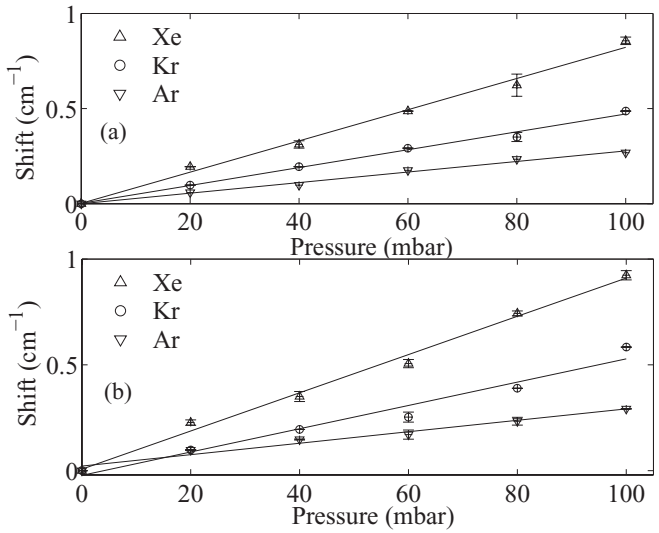

FIG. 5. Spectral line shift as a function of noble gas pressure for (a) Ba[$5d_{3/2}19d$] $J = 0$, and (b) Ba[$5d_{3/2}19d$] $J = 2$, autoionizing states.

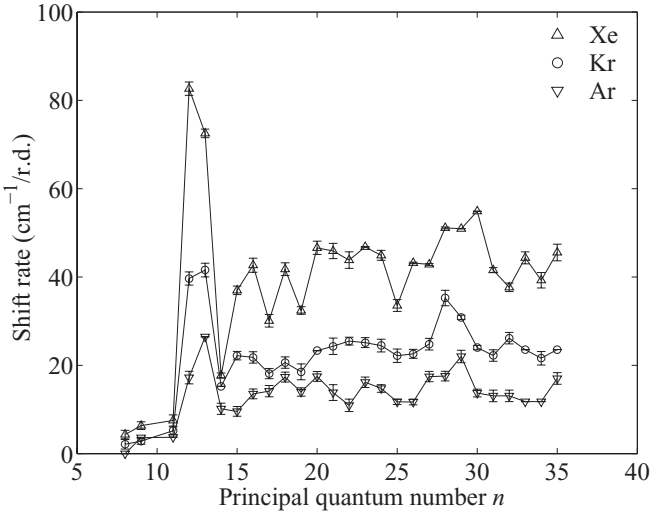

FIG. 6. Line shift (per r.d.) of the $5d_{3/2}nd\ ^1D_0$ series of barium due to collision with various inert gases as a function of principal quantum number.

line shifts on foreign gas pressure for the autoionizing lines presented in Fig. 5 is similar to that of Rydberg series below the first ionization limit [10].

The shift rates per relative density (in cm^{-1}/r.d.) of the resonance lines of the $5d_{3/2}nd\ ^1D_J$ series for $J = 0$ and $J = 2$ at a fixed perturber pressure of 100 mbar for different gases are represented in Table I and Table II, respectively (columns 4, 5, and 6). As the absolute shift depends on the number density of perturber gases, the shift rates were calculated per relative density (1 r.d. $= 2.687 \times 10^{19}$ atoms/cm^{-3}) in amagat units defined by

$$\text{r.d.} = \frac{p}{760}\frac{273}{T}\ (\text{amagat}),$$

where p is the pressure in torr and T is the temperature in Kelvin. If we consider a perturber gas pressure of 100 mbar and a cell temperature of 800 °C, the measured shift values should be divided by 0.025 for conversion to shift rate in cm^{-1} (r.d.)$^{-1}$. The reported shift rates are the average of five experimental trials, and error values given in Tables I and II are the standard errors calculated using standard deviation from the mean values. In places where the error is reported as 0.0 the calculated errors were less than 0.05 cm^{-1}/r.d. Plots of shift rates in terms of principal quantum number n are given in Fig. 6 for $J = 0$ and in Fig. 7 for $J = 2$. In both graphs, shift rates for different members of the series increase in the order of Ar, Kr, and Xe perturbers. The autoionizing states are coupled to other states, usually the $6s\varepsilon l$ continuum state; hence they are admixtures of two states. The continuum state electron is more easily perturbed by the colliding atoms. Therefore, the shift values for most states are greater than those obtained from the Fermi's model (electron scattering). The inverse of this effect has been observed for normal doubly excited states of barium. In this case, whenever the perturbed state has an admixture of a low-lying state the shift rate decreases. This is because most of the time the valence electron is not influenced by the colliding atom; hence a smaller net shift is observed.

As seen in Figs. 6 and 7, shift rates of the resonance lines show a significant rise for $11 < n < 14$. In this range of

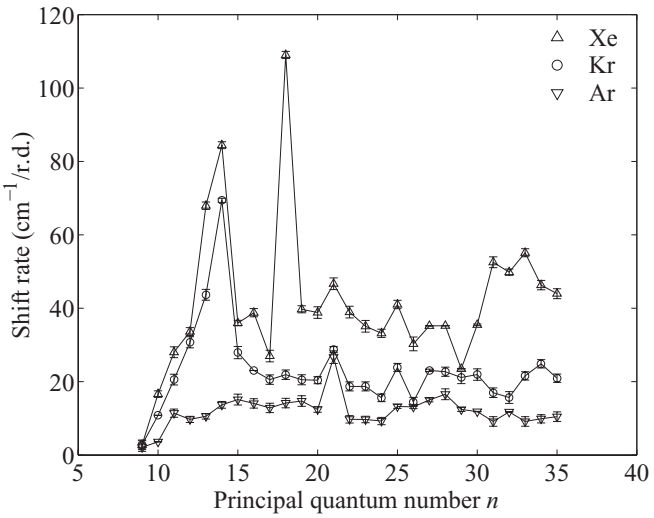

FIG. 7. Line shift (per r.d.) of the $5d_{3/2}nd\ ^1D_2$ series of barium due to collision with various inert gases as a function of principal quantum number.

n the series coincides in energy with the $6p^2$ configuration and therefore the interconfiguration interaction explains the rise of the shift rates. This interaction can be considered as state changing inelastic scattering of the Rydberg electron by the perturber atom—which, in the absence of coinciding configurations (such as $6p^2$ in this case), does not contribute to energy shifts [2]. The perturbation due to interaction of $5d_{3/2}nd$ and $6p^2$ configurations is the most significant both in $J = 0$ and $J = 2$. However, as observed in Figs. 6 and 7, there are other interactions that happen over a smaller energy range which cause the shift of a single line only. One such example is the shift rate of $5d_{3/2}18d$. Although the shift rate of this member of the series with $J = 0$ is not too different from its neighbors, for $J = 2$ and with Xe perturber a significant shift in the position of this line is observed.

A possible explanation is offered when comparing the line shifts due to $6p^2$ configuration and the shift of $5d_{3/2}18d$, $J = 2$. In the former case, the competing states of $6p^2$ configuration happen over hundreds of wave numbers [18] (more than 30 nm in wavelength); hence, several members of the $5d_{3/2}nd$ series are affected by the corresponding perturbation. This implies the existence of a sharp resonance near the position of $5d_{3/2}18d$, $J = 2$. The interaction between these two competing resonances must be weak, which explains the absence of line shifts with Ar and Kr perturbers. A stronger perturbation coming from Xe with larger scattering length and polarizability is needed to observe this interaction.

Except strong fluctuations due to configuration mixings, the overall variation of line shifts versus the principal quantum number given in Figs. 6 and 7 is comparable to that of other Rydberg series. In the Rydberg series below the first ionization limit the shift rate increases with increasing n and reaches a plateau for high n values [2,11]. For the autoionizing series large fluctuations superimpose a similar trend that indicates the highly interactive nature of the autoionizing states as explained above.

IV. CONCLUSION

The resonance spectral lines of the $5d_{3/2}nd\ ^1D_{0,2}$, $n > 7$, autoionizing series of Ba were known for $n \leqslant 30$. The series members energies were measured in this paper for $30 < n < 65$. The line shapes of the spectral lines obtained from two-photon absorptions were studied, and the energy shift of these lines induced by rare gas pressures were also investigated. Being above the first ionization limit, the autoionizing lines when under collisions with noble atoms, show different behavior compared to those Rydberg states below the ionization limit. The dependence of the line shift on the principal quantum number and the broadened spectral line profiles reveal some of these differences. A detailed investigation of the line broadening for autoionizing states is underway, which will provide some information about the interatomic potential for the Rydberg atom-rare gas atom system. We hope these results will motivate more theoretical work toward understanding the physical processes involved in these collisions. Nevertheless, in the absence of theories, more experimental studies are needed to be able to understand the collisional dynamics of autoionizing energy states.

ACKNOWLEDGMENTS

We acknowledge the support of the Research Administration (RA) of Kuwait University through Project No. SP 01/04 and also through the General Facility Project, GS 03/01, from the Vice Dean of Research, Faculty of Science. The authors are grateful to Professor G. Pichler for his scientific input and help in writing this manuscript. We thank R. R. Nair (GS 01/08) and Z. Suji for their technical assistance during different stages of our experiments. Discussions with Dr. E. D. Davis from the Physics Department of Kuwait University were also helpful.

[1] J. P. Connerade, *Highly Excited Atoms* (Cambridge University Press, Cambridge, 1998).
[2] T. F. Gallagher, *Rydberg Atoms* (Cambridge University Press, Cambridge, 1994).
[3] W. E. Cooke, T. F. Gallagher, S. A. Edelstein, and R. M. Hill, Phys. Rev. Lett. **40**, 178 (1978).
[4] N. H. Tran, P. Pillet, R. Kachru, and T. F. Gallagher, Phys. Rev. A **29**, 2640 (1984).
[5] J. Berkowitz, *Photoabsorption, Photoionization, and Photoelectron Spectroscopy* (Academic Press, New York, 1979).
[6] J. R. Tolsma, D. J. Haxton, C. H. Greene, R. Yamazaki, and D. S. Elliott, Phys. Rev. A **80**, 033401 (2009).
[7] W. R. Hindmarsh, A. D. Petford, and G. Smith, Proc. R. Soc. A **297**, 296 (1967).
[8] K. Hornberger, S. Uttenthaler, B. Brezger, L. Hackermuller, M. Arndt, and A. Zeilinger, Phys. Rev. Lett. **90**, 160401 (2003).

[9] M. Shapiro and P. Brumer, Rep. Prog. Phys. **66**, 859 (2003).
[10] M. Marafi, Z. Suji, K. Bhatia, Y. Makdisi, and J. Mathew, J. Phys. B: At. Mol. Opt. Phys. **40**, 4211 (2007).
[11] M. Marafi, K. Afrousheh, Y. Makdisi, Z. Suji, and J. Mathew, J. Phys. B: At. Mol. Opt. Phys. **42**, 145003 (2009).
[12] P. Camus, M. Dieulin, A. El Himdy, and M. Aymar, Phys. Scr. **27**, 125 (1983).
[13] M. Aymar, P. Camus, and A. El Himdy, Phys. Scr. **27**, 183 (1983).
[14] T. J. Tseng and M. A. Whitehead, Phys. Rev A **24**, 16 (1981).
[15] X. Wang and W. E. Cooke, Phys. Rev. A **47**, 1778 (1993).
[16] X. Wang, J. G. Story, and W. E. Cooke, Phys. Rev. A **43**, 3535 (1991).
[17] R. M. Jopson, R. R. Freeman, W. E. Cooke, and J. Bokor, Phys. Rev. Lett. **51**, 1640 (1983).
[18] M. A. Kalyar, M. Rafiq, and M. A. Baig, Phys. Rev. A **80**, 052505 (2009).
[19] K. Niemax, Appl. Phys. B **38**, 147 (1985).
[20] M. Marafi, Z. Suji, K. Bhatia, and J. Mathew, J. Phys. B: At. Mol. Opt. Phys. **41**, 205203 (2008)